

Two-step model of fusion for the synthesis of superheavy elements

Caiwan Shen,^{1,2,3,4} Grigori Kosenko,^{4,5} and Yasuhisa Abe⁶

¹*China Institute of Atomic Energy, P.O. Box 275(18), 102413 Beijing, China*

²*INFN-LNS, I-95123 Catania, Italy*

³*Center of Theoretical Nuclear Physics, National Laboratory of Lanzhou, Lanzhou, China*

⁴*RIKEN, Wako, Saitama, Japan*

⁵*Department of Physics, University of Omsk, RU-644077 Omsk, Russia*

⁶*Yukawa Institute for Theoretical Physics, Kyoto University, 606-8502 Kyoto, Japan*

(Received 24 June 2002; published 30 December 2002)

A new model is proposed for fusion mechanisms of massive nuclear systems where so-called fusion hindrance exists. The model describes two-body collision processes in an approaching phase and shape evolutions of an amalgamated system into the compound nucleus formation. It is applied to ⁴⁸Ca-induced reactions and is found to reproduce the experimental fusion cross sections extremely well, without any free parameter. Combined with the statistical decay theory, residue cross sections for the superheavy elements can be readily calculated. Examples are given.

DOI: 10.1103/PhysRevC.66.061602

PACS number(s): 25.70.Jj, 24.60.-k, 25.60.Pj, 27.90.+b

How many elements exist in nature or what is the heaviest element have been intriguing questions since the Periodic Table was proposed for the chemical elements. The heaviest element that exists in nature is now known to be uranium with an atomic number Z of 92. But the discovery of the magic numbers in atomic nuclei and their understanding by the shells of nucleonic motion [1] suggest that much heavier atomic nuclei might exist, stabilized by extra bindings due to possible shells next to the largest ones known, i.e., $Z=82$ and $N=126$. Actually, many theoretical calculations have been made, predicting the next double closed shell nucleus to be with $Z=114$, 120, or 126 and $N=184$ [2]. Naturally, enormous experimental effort has been devoted to finding out traces of existence of the corresponding superheavy atomic nuclei and to synthesizing them with nuclear reactions, especially with heavy-ion fusion reactions [3]. But what combination of ions is favorable as entrance channels and what incident energy is the optimum for residues are not predicted well, and thus, the experiments have been performed according to the results of systematic studies done so far. This is due to the lack of knowledge of reaction mechanisms.

Based on the theory of compound nucleus reactions, the residue cross sections are given as follows:

$$\sigma_{\text{res}} = \pi \lambda^2 \sum_J (2J+1) \cdot P_{\text{fusion}}^J(E_{\text{c.m.}}) \cdot P_{\text{surv}}^J(E^*), \quad (1)$$

where λ is the inverse of the wave number and J is the total angular momentum quantum number. P_{fusion} and P_{surv} denote the fusion and the survival probabilities, respectively. The latter is given by the statistical theory of decay, i.e., by competitions between neutron emission and fission decay. Essentially unknown is the fusion probability, i.e., the fusion mechanism of massive systems, although there are ambiguities in the parameters in the properties of heavy and superheavy nuclei which give rise to uncertainties in calculating the survival probability.

In lighter systems, the fusion probability is well determined by the barrier defined with the Coulomb and nuclear

attraction between nuclei in the entrance channel, but in massive systems, the situation is not so simple. It has been well known experimentally that there is fusion hindrance [4], which is often described with so-called extra-push energy, which is required for a system to fuse in addition to the barrier height [5]. A physical origin or mechanism is not yet well clarified. There are two possible interpretations proposed. They both attribute it to energy dissipations; one is due to the dissipation of the initial kinetic energy during two-body collisions passing over the barrier [6], while the other is due to the dissipation of the energy of collective motions which would lead an amalgamated system to the spherical compound nucleus [5]. It is natural to consider that both mechanisms exist, though we do not know *a priori* which dominates in which situation. We, thus, propose a new theoretical framework for fusion, i.e., a two-step model which incorporates both of them properly [7].

In the approaching phase of passing over the Coulomb barrier, we describe the system as collision processes under frictional forces, up to the contact point of two incident nuclear matters, and then we describe dynamical evolutions of the amalgamated mononuclear system toward the spherical shape under frictional forces acting in collective motion of excited nuclei. As is given below, both dynamical processes are described by Langevin equations which include random forces associated to the respective frictions. It would be worth to mentioning here that the fluctuations due to the random forces are crucially important in problems of small probability such as in syntheses of the superheavy elements (SHE), because we have to investigate cases where mean trajectories never reach the spherical shape. Another point to be mentioned is that since the two steps are connected successively, the results of the first step not only give a probability for incident ions to stick to each other (sticking probability P_{stick}) but also give initial conditions for the second step. Thus, the method of the connection from the first to the second steps is natural, which is neither related to the diabaticity nor the adiabaticity. It is completely new and could be called “statistical,” as will be seen below. In massive sys-

tems, there is a conditional saddle point, or a ridge line between the amalgamated configuration and the spherical shape on the potential energy surface calculated with the liquid drop model (LDM), which could be considered to be another barrier inside and makes most trajectories return back to re-separation (quasifission, etc.), i.e., it gives rise to a small probability for forming the spherical shape (formation probability P_{form}). Thus, the fusion probability is given by the product of the two probabilities,

$$P_{\text{fusion}}^J(E_{\text{c.m.}}) = P_{\text{stick}}^J(E_{\text{c.m.}}) \cdot P_{\text{form}}^J(E_{\text{c.m.}}). \quad (2)$$

In order to realize the model, we employ the surface friction model (SFM) [8] for the approaching phase and the one-body wall-and-window formula [9] of the dissipation for the shape evolutions, i.e., for the second step.

As for the approaching phase, the equation of motion is only for the radial degree of freedom and the orbital angular momentum, and is given as

$$\begin{aligned} \frac{dr}{dt} &= \frac{1}{\mu} p, \\ \frac{dp}{dt} &= -\frac{dV}{dr} - \frac{\partial \hbar^2 L(t)^2}{\partial r} \frac{p}{2\mu r^2} - C_r(r) \frac{p}{\mu} + R_r(t), \\ \frac{dL(t)}{dt} &= -\frac{C_L(r)}{\mu} \cdot [L(t) - L_{st}] + R_T(t), \end{aligned} \quad (3)$$

where μ is the reduced mass of the collision system, and V is the sum of the Coulomb potential V_c and the nuclear potential V_n . $C_i(r)$ is the radial or the tangential friction coefficient which is assumed to have the following form factor, $C_i(r) = K_i^0 \cdot (dV_n/dr)^2$, where $K_r^0 = 0.035$ and $K_T^0 = 0.0001$ in units of 10^{-21} s/MeV. L_{st} denotes the limiting orbital angular momentum under the friction, which is the so-called sliding limit in the SFM and is equal to $5/7 \cdot L$. R_i denotes a random force associated with the friction for $i = r$ (radial) or T (tangential), and, assumed to be Gaussian, to satisfy the following property:

$$\begin{aligned} \langle R_i(t) \rangle &= 0, \\ \langle R_i(t) \cdot R_j(t') \rangle &= 2 \delta_{ij} \delta(t-t') \cdot C_i[r(t)] T^J(t), \end{aligned} \quad (4)$$

where the last equation is the fluctuation-dissipation theorem with temperature $T^J(t)$, J being equal to a total angular momentum of the system, i.e., an incident orbital angular momentum L . For the case of i and j equal to T (tangential), $r(t)^2$ is factored in the rhs of Eq. (4). We calculate many trajectories over relevant impact parameters and obtain probabilities for their reaching the contact point, respectively. Figure 1(a) shows the calculated sticking probability for the $L=0$ for the case of $^{48}\text{Ca}-^{238}\text{U}$ system. Incident energy is given relative to the barrier height. It is readily seen that at energies just above the barrier there is almost no probability. This is due to the fact that the form factor assumed in the SFM stretches over outside the barrier top position in massive systems. The results already appear to explain the fusion

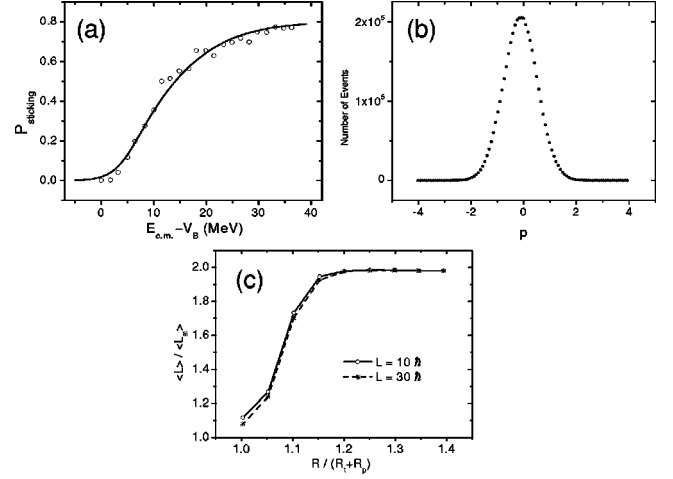


FIG. 1. Results on the $^{48}\text{Ca}-^{238}\text{U}$ system with the SFM. The sticking probability for $L=0$ is shown in (a) (curve is a guide for the eye), the radial momentum distribution in (b) in unit of 10^{-21} sec MeV/fm, and the average orbital angular momentum vs the relative distance is shown in (c).

hindrance and at least partially the extra-push energy, while the second step is also expected to give rise to an additional contribution. In order to know the physical situation at the contact point, we analyze the radial momentum distribution as well as that of the orbital angular momentum. The radial momentum distribution is found to be almost purely Gaussian, as shown in Fig. 1(b). Its width is consistent with the temperature of the heat bath of nucleons which is supposed to absorb the initial kinetic energy through the friction force. The example shown is for $L=0$, but the other angular momentum cases behave in the same way. Therefore, the calculated distribution $S^J(p_0, E_{\text{c.m.}})$ can be expressed as follows for each angular momentum:

$$S^J(p_0, E_{\text{c.m.}}) = P_{\text{stick}}^J(E_{\text{c.m.}}) \cdot g^J(p_0, \bar{p}_0^J, T_0^J), \quad (5)$$

where the normalized Gaussian distribution $g^J(p_0, \bar{p}_0^J, T_0^J)$ is given generally so as to include an average mean momentum left (\bar{p}_0^J), which is almost equal to zero in the present case. This distribution is used as the initial inputs to the dynamical evolutions in the second step, i.e., to Eq. (8) below. T_0^J denotes the temperature of the amalgamated system. The total energy available for the compound nucleus E^* is given by the energy conservation $E^* = E_{\text{c.m.}} + Q = V_0 - E_{\text{shell}} + \varepsilon_0 + k_0$, where Q denotes the Q value of the fusion reaction. E_{shell} is the shell correction energy of the ground state, V_0 the LDM potential energy of the contact point, ε_0 the intrinsic excitation, and k_0 the radial kinetic energy left at the contact point. The latter two are on average given as $a_0 \cdot T_0^{J2}$ and $(\bar{p}_0^J)^2/2\mu + \frac{1}{2}T_0^J$, respectively, with the level density parameter a_0 which is calculated according to Töke and Swiatecki [10]. The orbital angular momentum is also analyzed. The average value is plotted as a function of the radial distance in Fig. 1(c). It is seen that it approaches the dissipation limit L_{st} at about the contact point, which indicates that the incident system reaches the sticking limit, if the rolling friction is properly taken into account. We, thus, can consider that the relative motion is completely damped and reaches the ther-

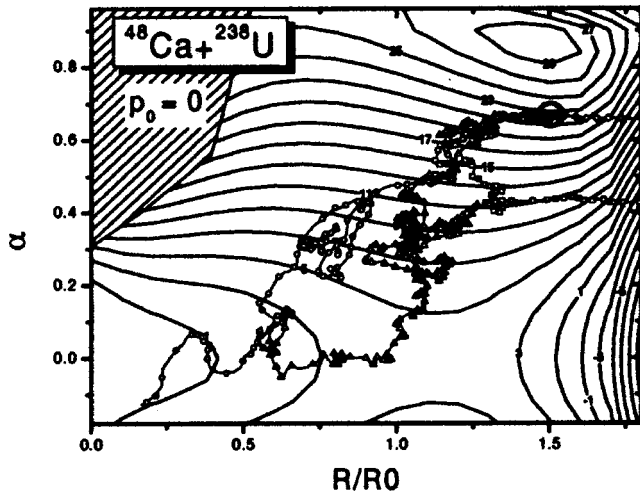


FIG. 2. Examples of the trajectories are displayed with the same initial radial momentum being equal to zero. Random force gives rise to a variety of the trajectories. The circle in the upper right corner corresponds to the touching configuration reached by the first step, from which dynamical evolutions of shape start (R_0 is the radius of the spherical ground state).

mal equilibrium with the heat bath at the contact point, i.e., that the incident ions form an amalgamated mononuclear system, the probability of which depends on the incident energy and is extremely small just above the barrier. It should be noticed here that $\bar{p}_0^J = 0$ does not always hold, for example, it does not in the $^{100}\text{Mo}-^{100}\text{Mo}$ system.

Subsequent shape evolutions of the pear-shaped mononucleus formed with the incident ions are described by the multidimensional Langevin equation which is the same as that used for dynamical studies of fission [11],

$$\begin{aligned} \frac{dq_i}{dt} &= (m^{-1})_{ij} \cdot p_j, \\ \frac{dp_i}{dt} &= -\frac{\partial U^J}{\partial q_i} - \frac{1}{2} \frac{\partial}{\partial q_i} (m^{-1})_{jk} \cdot p_j \cdot p_k \\ &\quad - \gamma_{ij} \cdot (m^{-1})_{jk} \cdot p_k + g_{ij} \cdot R_j(t), \\ g_{ik} g_{jk} &= \gamma_{ij} \cdot T^J, \end{aligned} \quad (6)$$

where summation is implicitly assumed over repeated suffixes. The collective mass tensor m_{ij} is the hydrodynamical one and the potential U^J is calculated by the finite range LDM with two-center parametrization of nuclear shapes [12], added with the rotational energy of the system calculated with the rigid body moment of inertia. The random force $R_i(t)$ is again Gaussian with the normalization 2, and the tensor g_{ij} is now related to the friction tensor γ_{ij} , as is given in the last equation, i.e., the generalized fluctuation-dissipation theorem in the multidimensional case. The friction tensor is calculated with the wall-and-window formula [9]. The temperature T^J of the heat bath is better taken to be that at the conditional saddle point, but is approximated with that at the contact point, i.e., T_0^J . They are close to each

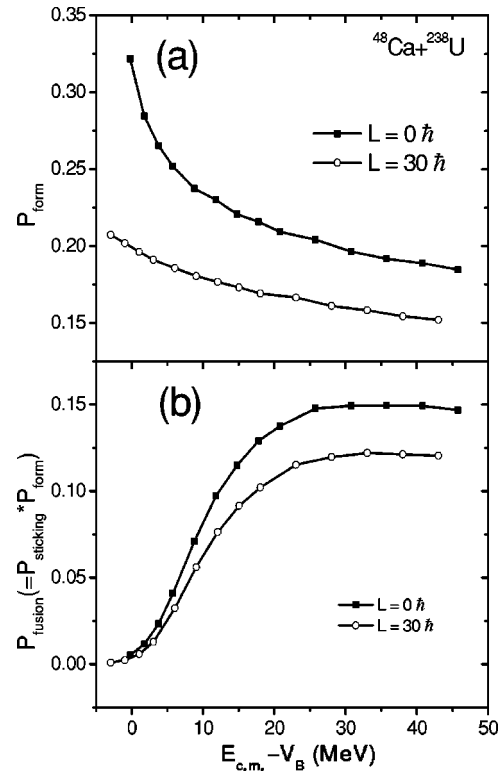


FIG. 3. Calculated formation and fusion probabilities are shown in (a) and (b), respectively.

other for the ^{48}Ca -induced reactions. In the present calculations we only use the relative distance R and the mass asymmetry coordinate α with the other degrees of freedom being frozen. For example, the neck parameter is taken to be 0.8, based on our experience that it does not change very much while passing over the conditional saddle point in the three-dimensional calculations. Figure 2 shows examples of the trajectories on the LDM potential for the $^{48}\text{Ca}-^{238}\text{U}$ system for initial radial momenta and thus initial energies equal to zero (the initial value of α is taken always to be zero, because the SFM does not include the α degree of freedom). Calculations of many trajectories, starting with various initial radial momenta, give a distribution of formation probability $F^J(p_0, T^J)$. By making it a convolution with the Gaussian distribution of the initial momentum $g^J(p_0, \bar{p}_0^J, T_0^J)$, we obtain the formation probability P_{form} :

$$P_{\text{form}}(E_{\text{c.m.}}) = \int dp_0 F^J(p_0, T^J) \cdot g^J(p_0, \bar{p}_0^J, T_0^J). \quad (7)$$

Figure 3(a) shows the calculated formation probability for the $^{48}\text{Ca}-^{238}\text{U}$ system for $L=0$ and 30. In Fig. 3(b), the final fusion probability is plotted versus incident energy. At first glance, the decreasing energy dependencies seem to be peculiar, but the energy dependence of the passing-over probability under friction delicately depends on the strength of friction and the incident momentum. Actually, slightly weaker friction gives rise to an increasing energy dependence. A detailed analysis with the one-dimensional model

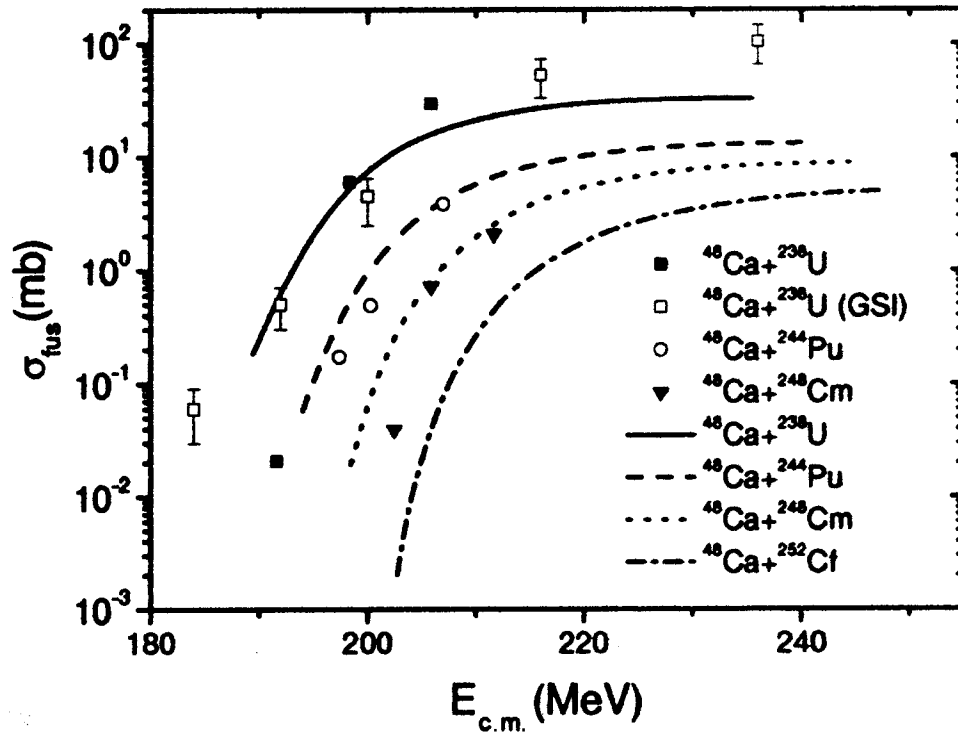


FIG. 4. Calculated excitation functions of fusion reactions for $^{48}\text{Ca}-^{238}\text{U}$, $^{48}\text{Ca}-^{244}\text{Pu}$, $^{48}\text{Ca}-^{248}\text{Cm}$ and $^{48}\text{Ca}-^{252}\text{Cf}$ systems, together with the available experimental data (Ref. [13]) for GSI and for Dubna (Ref. [14]).

will be given elsewhere [15]. It should be also mentioned here that the present model is completely classical, and thus there is no quantum tunneling effect included, which limits the lowest energy to be covered.

Fusion cross sections are calculated with the fusion probability as usual, $\sigma_{\text{fusion}} = \pi\lambda^2 \sum_j (2J+1) \cdot P_{\text{fusion}}^j(E_{\text{c.m.}})$, and are shown in Fig. 4 for the four systems with a ^{48}Ca beam, together with some measured cross sections [14]. It is extremely surprising that the calculations well reproduce the experiments without any adjustment of the model parameters. Experimental measurements are highly desirable on the $^{48}\text{Ca}-^{252}\text{Cf}$ system for comparison with the present calculations.

In order to show that we are ready for calculations of residue cross sections for SHE, we give examples for Z

$=114, 116,$ and 118 , by the use of P_{surv} calculated with HIVAP [16]. Actually, the shell correction energies are the most crucial quantities in residue calculations, because they effectively give the fission barriers for SHE. Since they are not yet firmly predicted, we thus take those by Möller *et al.* [17] and Liran [18] as typical examples of mass predictions, and compare with the recent Dubna experiments [19], which are given in Table I.

In brief, the new two-step model has been found to be extremely successful in reproducing the available fusion data of ^{48}Ca -induced reactions. By combining the present fusion probabilities with the standard statistical decay calculations, we have obtained residue cross sections for $Z=114, 116,$ and 118 , which are in reasonable agreement with the recent Dubna experiments, but with rather small shell correction

TABLE I. Calculated maximum residue cross sections of the three systems $^{48}\text{Ca}-^{244}\text{Pu}$, $^{48}\text{Ca}-^{248}\text{Cm}$, and $^{48}\text{Ca}-^{252}\text{Cf}$ are summarized. The factor 1/3 for Möller masses is rather arbitrarily chosen ($\sigma_{\text{max}}:pb, E^*:MeV$).

^{48}Ca	Prediction of		$3n$		$4n$	
	ΔE_{shell} (MeV)	σ_{max}	E^*	σ_{max}	E^*	
^{244}Pu	Liran	-0.23	0.018	30.6	0.018	36.5
	Möller/3	-2.96	7.39	30.1	6.00	35.3
	experiment		≈ 1	$E_{\text{lab}}=236$	≈ 1	$E_{\text{lab}}=236$
^{248}Cm	Liran	-1.37	0.254	31.1	0.045	37.8
	Möller/3	-2.86	4.56	30.4	2.98	35.6
	experiment				0.6	35.8
^{252}Cf	Liran	-3.24	1.057	32.7	0.095	38.2
	Möller/3	-2.41	0.216	28.8	0.086	33.5

energies, much smaller than previously thought. A systematic study of residue cross sections are being made. Furthermore, the model is now being applied to other massive systems, such as ^{100}Mo - ^{100}Mo , etc.

This work was partly supported by the Chinese Academy of Science Knowledge Innovation Project (Grant No. KJCX1-N11) and by the Grant-in-Aid of JSPS (Grant No. 13640278).

-
- [1] M.G. Mayer and J.H.D. Jensen, *Elementary Theory of Nuclear Shell Structure* (Wiley, New York, 1955).
- [2] P. Möller and R. Nix, *J. Phys. G* **20**, 1681 (1994); S. Cwiok *et al.*, *Nucl. Phys. A* **611**, 211 (1996); M. Bender *et al.*, *Eur. Phys. J. A* **7**, 467 (2000).
- [3] S. Hofmann, *Rep. Prog. Phys.* **61**, 639 (1999); P. Armbruster, *Annu. Rev. Nucl. Part. Sci.* **50**, 411 (2000).
- [4] A.B. Quint *et al.*, *Z. Phys. A* **346**, 199 (1993).
- [5] W.J. Swiatecki, *Phys. Scr.* **24**, 113 (1981); S. Bjornholm and W.J. Swiatecki, *Nucl. Phys. A* **391**, 471 (1982).
- [6] P. Fröbrich *et al.*, *Nucl. Phys. A* **406**, 557 (1983).
- [7] Analytic study with the one-dimensional model is reported in Y. Abe *et al.*, *Proceedings YKIS01* [*Prog. Theor. Phys. Suppl.* **146**, 104 (2002)].
- [8] D.H.E. Gross and H. Kalinowski, *Phys. Rep.* **45**, 175 (1978); see also R. Bass, *Nuclear Reactions With Heavy Ions* (Springer, Berlin, 1980), Chap. 7.
- [9] J. Blocki *et al.*, *Ann. Phys. (N.Y.)* **113**, 330 (1978).
- [10] J. Töke and W.J. Swiatecki, *Nucl. Phys. A* **372**, 141 (1981).
- [11] T. Wada *et al.*, *Phys. Rev. Lett.* **70**, 3538 (1993); Y. Abe *et al.*, *Phys. Rep.* **275**, 49 (1996).
- [12] K. Sato *et al.*, *Z. Phys. A* **290**, 145 (1979).
- [13] W.Q. Shen *et al.*, *Phys. Rev. C* **36**, 115 (1987).
- [14] M.G. Itkis *et al.*, *Nuovo Cimento A* **111A**, 783 (1998).
- [15] D. Boilley, J.D. Bao, and Y. Abe (unpublished).
- [16] W. Reisdorf (private communication).
- [17] P. Möller *et al.*, *At. Data Nucl. Data Tables* **59**, 185 (1995).
- [18] S. Liran, A. Marinov, and N. Zeldes, *Phys. Rev. C* **62**, 047301 (2000).
- [19] Yu. Oganessian *et al.*, *Phys. Rev. Lett.* **83**, 3154 (1999); *Nucl. Phys. A* **682**, 108c (2001).